American Journal of Pathology, Vol. 159, No. 1, July 2001

Primary Renal Neoplasms with the *ASPL-TFE3* Gene Fusion of Alveolar Soft Part Sarcoma

A Distinctive Tumor Entity Previously Included among Renal Cell Carcinomas of Children and Adolescents

Pedram Argani,* Cristina R. Antonescu,‡‡ Peter B. Illei,‡‡ Man Yee Lui,‡‡ Charles F. Timmons,† Robert Newbury,‡ Victor E. Reuter,‡‡ A. Julian Garvin,§ Antonio R. Perez-Atayde,¶‖ Jonathan A. Fletcher,¶‖ J. Bruce Beckwith,** Julia A. Bridge,†† and Marc Ladanyi‡‡

From the Department of Pathology, The Johns Hopkins Hospital, Baltimore, Maryland; the Department of Pathology,† Children's Medical Center, Dallas, Texas; the Department of Pathology,‡ Children's Hospital San Diego, California; the Department of Pathology,§ Baptist Medical Center–Wake Forest University, Winston-Salem, North Carolina; the Department of Pathology,¶ Children's Hospital and Brigham and Women's Hospital, Boston, Massachusetts; the Department of Pathology,‖ Harvard Medical School, Boston; the Department of Pathology,** Loma Linda University, Loma Linda, California; Departments of Pathology, Pediatrics, and Orthopaedic Surgery,†† University of Nebraska Medical Center, Omaha, Nebraska; and the Department of Pathology‡‡ Memorial Sloan-Kettering Cancer Center, New York, New York*

The unbalanced translocation, der(17)t(X;17)(p11.2;q25), is characteristic of alveolar soft part sarcoma (ASPS). We have recently shown that this translocation fuses the *TFE3* transcription factor gene at Xp11.2 to *ASPL,* a novel gene at 17q25. We describe herein eight morphologically distinctive renal tumors occurring in young people that bear the identical *ASPL-TFE3* fusion transcript as ASPS, with the distinction that the t(X;17) translocation is cytogenetically balanced in these renal tumors. A relationship between these renal tumors and ASPS was initially suggested by the cytogenetic finding of a balanced t(X;17)(p11.2;q25) in two of the cases, and the *ASPL-TFE3* fusion transcripts were then confirmed by reverse transcriptase-polymerase chain reaction. The morphology of these eight *ASPL-TFE3* fusion-positive renal tumors, although overlapping in some aspects that of classic ASPS, more closely resembles renal cell carcinoma (RCC), which was the *a priori* diagnosis in all cases. These tumors demonstrate nested and pseudopapillary patterns of growth, psammomatous calcifications, and epithelioid cells with abundant clear cytoplasm and well-defined cell borders. By immunohistochemistry, four tumors were negative for all epithelial markers tested, whereas four were focally positive for cytokeratin and two were reactive for epithelial membrane antigen (EMA) (one diffusely, one focally). Electron microscopy of six tumors demonstrated a combination of ASPS-like features (dense granules in four cases, rhomboid crystals in two cases) and epithelial features (cell junctions in six cases, microvilli and true glandular lumens in three cases). Overall, although seven of eight tumors demonstrated at least focal epithelial features by electron microscopy or immunohistochemistry, the degree and extent of epithelial differentiation was notably less than expected for typical RCC. We confirmed the balanced nature of the t(X;17) translocation by fluorescence *in situ* hybridization in all seven renal tumors thus analyzed, which contrasts sharply with the unbalanced nature of the translocation in ASPS. In summary, a subset of tumors previously considered to be RCC in young people are in fact genetically related to ASPS, although their distinctive morphological and genetic features justify their classification as a distinctive neoplastic entity. Finally, the finding of distinctive tumors being associated with balanced and unbalanced forms of the same translocation is to our knowledge, unprecedented. *(Am J Pathol 2001, 159:179–192)*

We have recently identified the gene fusion resulting from the chromosome translocation that is characteristic of alveolar soft part sarcoma (ASPS), der(17)t(X;17)(p11.2;

Supported in part by the Alliance Against Alveolar Soft Part Sarcoma (ML).

Accepted for publication April 13, 2001.

Address correspondence or reprint requests to Marc Ladanyi, M.D., Memorial Sloan-Kettering Cancer Center, Department of Pathology, 1275 York Ave., New York, NY 10021. E-mail: ladanyim@mskcc.org or to Pedram Argani, M.D., The Johns Hopkins Hospital, Surgical Pathology Weinberg Building, Room 2242, 401 N. Broadway, Baltimore, MD 21231-2410. E-mail: pargani@jhmi.edu.

q25).[1] This unbalanced translocation results in the fusion of the *TFE3* gene on Xp11.2, a member of the basic-helix-loop-helix family of transcription factors, to a novel gene named *ASPL* on 17q25.[1] The resulting fusion gene encodes chimeric *ASPL-TFE3* RNA transcripts. Two mutually exclusive types of fusion products, designated type 1 and type 2, are observed. They differ in their exon composition, reflecting, respectively, the exclusion or inclusion of *TFE3* exon 3 in the *ASPL-TFE3* fusion transcript. *TFE3* was previously found to be rearranged by specific reciprocal translocations involving Xp11.2 in a subset of pediatric renal cell carcinomas (RCCs).[2,3] In most of these cases, the translocation partner is a novel gene designated *PRCC* at 1q21.2, whereas in others, *TFE3* fuses instead with the splicing factor genes, *PSF* at 1p34 or *NonO* at Xq12.[4] *ASPL* shows no sequence similarities to *PRCC*, *PSF*, or *NonO*.

Of note, other variant translocations involving Xp11.2 have been identified in tumors reported as RCCs. These include four published reports of pediatric renal carcinomas with a balanced t(X;17)(p11.2;q25), the breakpoints of which are cytogenetically identical to the translocation now recognized to be characteristic of ASPS.[5–8] Intriguingly, ASPS is well known to be capable of mimicking RCC morphologically, in that both tumors feature nested and alveolar patterns of growth bounded by prominent sinusoidal vasculature, and both contain polygonal cells with clear-eosinophilic cytoplasm and distinct borders.[9–12] Given these morphological similarities and the cytogenetic findings, we hypothesized that such renal tumors might in fact be related to ASPS.

Therefore, we have reviewed several of these reported carcinomas, along with cases coded as RCC in the files of two of the authors (JBB, VER), with the aim of identifying tumors bearing the *ASPL-TFE3* gene fusion characteristic of ASPS. We report herein the clinical, pathological, and genetic features of eight primary renal neoplasms in which we have identified the *ASPL-TFE3* fusion.

Materials and Methods

Study Group

We initially searched the files of the National Wilms Tumor Study Pathology Center (NWTSPC) and the affiliated consultation files of JBB for cases of carcinoma with available cytogenetic results. Two cases with a documented t(X;17)(p11.2;q25) were identified; one of these cases[7] was one of four previously published cytogenetic reports of RCC with a t(X;17), as noted above. Fresh frozen tissue suitable for RNA extraction for reverse transcriptase-polymerase chain reaction (RT-PCR) analysis was available from both tumors. Based on the morphological features of these two tumors that were noted to be distinctive and virtually identical (see Results), we reviewed all renal carcinomas in the files of JBB (~80 cases) and all cases classified as either clear cell RCC, papillary RCC, or unclassifiable RCC in the files of Memorial Sloan-Kettering Cancer Center (MSKCC) from 1990 to 1998 (~400 cases, compiled by VER) with the goal of identifying morphologically similar cases for which fresh frozen tissue was available. Cases 3 to 7 were identified in this search. Of note, cases 4 and 7 were initially reported as pediatric papillary renal carcinomas with voluminous cytoplasm, with the former bearing a translocation originally reported as der(X)t (X;7)(p11;q11) (see Results).[13] Case 8 is an additional anecdotal case identified recently by one of the authors (AJG). Clinical follow-up was obtained from the referring pathologist in each case.

Immunohistochemistry

After morphological identification of the cases, immunohistochemical labeling was performed on all eight cases at The Johns Hopkins Hospital on a single formalin-fixed, paraffin-embedded tissue block from each case. Briefly, 4-μm sections were deparaffinized in xylene for 30 minutes and rehydrated using graded ethanol concentrations. Antigen retrieval was performed using either protease digestion or steaming. Immunohistochemical labeling using the avidin-biotin peroxidase complex technique and 3′, 3′-diaminobenzidine as chromagen was performed with the automated Biotek-1000 staining system (Ventana/Biotek Solutions, Inc., Tucson, AZ). The antibodies used, vendors, pretreatments, and dilutions were as follows: EMA (DAKO, Carpinteria, CA; steam, 1:1000), desmin (DAKO; steam, 1:20,000), S100 protein (DAKO; steam, 1:6000), cytokeratin 7 (DAKO; protease, 1:50), vimentin (Zymed, San Francisco, CA; steam, 1:100), cytokeratin AE1/AE3 (Boehringer Mannheim, Indianapolis, IN; protease, 1:2000), cytokeratin Cam5.2 (Becton Dickinson, San Jose, CA; protease, prediluted), and HMB45 (DAKO; steam, 1:125). The rationale for applying this panel of antibodies is as follows. The combination of cytokeratin cocktail AE1/AE3 (which recognizes cytokeratins 1 to 8, 10, 14/15, 16, and 19) and cytokeratin cocktail Cam5.2 (which recognizes cytokeratins 8, 18, and 19) was chosen because it is a highly sensitive and well-recognized screen for cytokeratin expression.[14–16] Stains for cytokeratin 7 and EMA were performed because of their known reactivity with papillary RCC.[14,17] Stains for vimentin were performed chiefly for the purpose of documenting the immunoreactivity of the tissue section used, as evidenced by strong immunoreactivity of the intratumoral capillaries. Stains for S100 protein, HMB45 and desmin were performed to exclude melanoma, angiomyolipoma, and myogenic sarcomas. Stains for EMA and cytokeratin AE1/AE3 were repeated on all cases using the DAKO Envision system to eliminate the possibility of biotin-related artifactual staining.

Electron Microscopy

Ultrastructural studies were performed at MSKCC (by CRA) on representative tumor tissue obtained from either paraffin blocks or from fresh tumor. Tissue removed from the paraffin block was cut into small pieces. The pieces were soaked in xylene, with several changes, for 1 week. After this, the pieces were placed in 100% alcohol, then rehydrated through graded alcohols (100, 95, 80, 70, to

50%) for at least one-half hour each. Tissue was then soaked in buffer for one-half hour or until the tissue was osmicated. Representative fresh tumor tissue was fixed in 2% glutaraldehyde, postfixed in 1% osmium tetroxide, and embedded in epoxy resin using standard procedures. In each case, thick sections were cut and stained with toluidine blue from four embedded tissue blocks to select blocks suitable for ultrastructural evaluation. Thin sections were stained with uranyl acetate followed by lead citrate and examined with a Philips EM401 electron microscope (Eindhoven, The Netherlands).

Molecular Analysis

Molecular studies were performed at MSKCC on snap-frozen tumor tissue in seven cases, or frozen short-term primary culture (one case). RNA extraction was performed from frozen tissue using a standard organic extraction method (Trizol; Life Technologies, Inc., Friendsworth, TX).[18] To assess the adequacy of RNA for analysis, RT-PCR was performed using primers spanning an intron of the ubiquitously expressed phosphoglycerate kinase (*PGK*) gene, resulting in amplification of a 247-bp fragment, as described in detail elsewhere.[19] RNA samples in which the *PGK* product could not be demonstrated were considered inadequate for *ASPL-TFE3* analysis. Negative controls lacking RNA were included in all RT-PCR assays. The amplified fragments were identified by their size on agarose gel electrophoresis. The specificity of all positive results was further confirmed by negative controls containing the target RNA but lacking RT.

To detect the presence of an *ASPL-TFE3* fusion transcript, we performed RT-PCR using a forward primer from *ASPL* (AAAGAAGTCCAAGTCGGGCCA) and a *TFE3* exon 4 reverse primer (CGTTTGATGTTGGGCAGCTCA), as previously described.[1] RT-PCR for the reciprocal fusion product, *TFE3-ASPL*, was performed using an *ASPL* reverse primer (CACCGTCAGCTCAAAGAACTC) and a *TFE3* forward primer appropriate to the type of *ASPL-TFE3* rearrangement in each case: for cases with a type 1 *ASPL-TFE3* fusion, a *TFE3* exon 3 forward primer (TTGATGATGTCATTGATGAGATC), and in cases with a type 2 *ASPL-TFE3* fusion, a more upstream *TFE3* primer (GCTCAAAAGCCAACCCTTAC). The *ASPL* cDNA sequence and junctional sequences of both types of *ASPL-TFE3* fusion transcripts have been deposited in GenBank (accession numbers AF324219, AY034077, AY034078).

Fluorescence in Situ *Hybridization (FISH)*

FISH studies were performed at MSKCC on cytological touch preparations of frozen tissue of nine ASPS specimens (including cases ASPS-1 to 7, and ASPS-11, from our previous study,[1] and an additional case, ASPS-13) and six renal tumors (cases 1, 2, 3, 5, 6, and 8), and on cells of a primary culture of one additional renal tumor (case 4). We used two probes in a bicolor FISH assay: the RPC11 human bacterial artificial chromosome (BAC) clone 525L23 (Research Genetics, Huntsville, AL) in combination with the centromere 17-specific alphoid sequence probe [CEP 17 (Vysis, Downer's Grove, IL)]. On the current version of the human genome sequence GenBank Map (at www.ncbi.nlm.nih.gov/), BAC 525L23 maps to 17q25.3 telomeric to BAC RPC11–498C9 that by our previous sequence analysis is known to contain *ASPL*.[1] The map location of BAC 525L23 telomeric to *ASPL* is confirmed by our FISH results in ASPS cases (see below). One μg of each DNA probe was directly labeled with SpectrumOrange or SpectrumGreen using a nick translation kit according to the manufacturer's instructions (Vysis). The labeled DNA was then co-precipitated for annealing purposes with 2 μg of Cot-1 DNA (sonicated total human DNA). The chromosomal and telomeric location of the 525L23 BAC probe was first confirmed by hybridizing to metaphase spreads of normal human lymphocytes in a bicolor assay with CEP17. Interphase FISH studies on the ASPS and renal cases were then performed with the same combination of the CEP17 and 525L23 BAC probes. Bicolor FISH studies, whether metaphase or interphase, were performed as follows. The slides to be hybridized were pretreated with collagenase H (0.01% in Kreb's ringer at 37°C for 15 minutes) followed by formaldehyde postfixation [2% (v/v) in MgCl2 phosphate-buffered saline (PBS) for 10 minutes at room temperature], and followed by incubation in 2 mg/ml glycine-PBS. The slides were then prehybridized in 2× standard saline citrate (37°C for 30 minutes) and air-dried. Subsequently, the slides were denatured in 70% formamide, 2× standard saline citrate, pH 7.3, at 73 to 74°C for 6 minutes and placed immediately into cold 70% EtOH, followed by a cold ethanol series of 80, 90, and 100%. The slides were then placed on a slidewarmer for 1 minute at 45°C before hybridization. The probes were denatured at 73 to 74°C for 5 minutes. The cells and probes were sealed under an 18- × 18-mm coverslip and incubated for 16 to 18 hours at 37°C in a humidity chamber. Images were prepared using the Applied Image Analysis System (Applied Imaging, Pittsburgh, PA). The number of hybridization signals for each probe was assessed in a minimum of 200 interphase nuclei with strong and well-delineated signals. As negative controls, normal peripheral-blood lymphocytes were simultaneously hybridized with these probes.

Results

Clinical Features

The features of the eight cases are summarized in Table 1. There were five females and three males. The patients ranged from 17 months to 17 years of age. Three of the children with smaller tumors (cases 1, 3, and 8) presented with hematuria, whereas another patient with a small tumor (case 4) presented with a urinary tract infection. Two of the patients with larger tumors (cases 2 and 5) presented with abdominal masses. Patient 7 presented with flank pain.

Table 1. Renal *ASPL-TFE3* Cases in Present Series

Case	Age/sex	Presentation	Diameter	Stage	Immunostains for epithelial markers			
					AE1/3	CAM	CK7	EMA
1	8/F	Urinary tract infection→right renal mass	3.3 cm	NWTS stage 1, AJCC stage I (pT1N0M0)	–	–	–	–
2†	2/M	Enlarging abdominal girth→left renal mass	10.1 cm	NWTS stage 3, AJCC stage IV (pT4N1MX)‖	–	–	–	–
3	7/F	Hematuria→right renal mass	3.5 cm	NWTS stage 3, AJCC stage III (pT3aN1M0)	–	–	–	–
4‡	17/F	Hx of t(9;11) AML Hematuria→left renal mass	2.7 cm	NWTS stage 3, AJCC stage III (pT1N1MX)	+f	–	–	–
5	17/M	Flank Mass→right renal mass	8 cm	NWTS stage 3, AJCC stage III (pT3aNXM0)	+f	+f	+f	–
6	17/F	Retroperitoneal tumor	14 cm	NWTS stage 4, AJCC stage IV (pT4N1M1) (vertebral metastases)	+f	+f	+f	+d
7‡	15/F	Flank pain→right renal and retroperitoneal tumor	2.3 cm	NWTS stage 3, AJCC stage IV (pT4NXM0)‖	–	–	–	–
8	4/M	Hematuria→right renal mass	4 cm	NWTS stage 3, AJCC stage III (pT3aN1M0)	+f	–	+f	+f

Gross Pathological Features

Primary tumor diameters ranged from 2.3 to 14 cm. On cut surface, the tumors appeared to be soft and well circumscribed, with four described as tan, two as yellow, and one as pink. Five tumors were noted to be necrotic, whereas three demonstrated hemorrhagic foci. Five of the eight tumors demonstrated capsular penetration. No tumor involved the renal vein grossly. One tumor (case 7) arose in a kidney bearing a duplicated collecting system. No other abnormalities of the nonneoplastic kidneys were noted.

Light Microscopic Features

The morphological features of these eight tumors were similar, and therefore they are described together. All tumors appeared well circumscribed but unencapsulated at low power. Their basic architecture was organoid, with variably sized nests of tumor cells separated by delicate, thin fibrovascular septa (Figure 1). In some foci, the nests were solid and the fibrovascular septa were thin and inapparent giving rise to a sheet-like growth pattern (Figure 2). Although cells in the larger nests were focally dyscohesive, giving rise to the alveolar pattern, the septal vessels generally did not demonstrate the sinusoidal dilation usually associated with ASPS. In seven of the eight cases, foci of hemorrhage within the nests yielded a morphological appearance typically associated with clear cell RCC.[20]

The septa delineating the larger nests often did not connect, creating a pseudopapillary pattern as tumor cells clung to the branching fibrovascular septa (Figure 3). Unlike true papillae, these pseudopapillae generally demonstrated an irregular luminal border, and the nuclei were not aligned abluminally. Alternatively, large nests contained cross-sections of fibrovascular septa, to which occasional tumor cells clung. Such fibrovascular septa were often hyaline, and were associated with psammomatous calcifications in every case. Case 6 focally demonstrated trabecular and cribriform growth patterns with smooth luminal borders and extensively branching papillae, highly suggestive of true epithelial differentiation (Figure 4).

On high-power examination, tumor cells contained voluminous cytoplasm that was sharply demarcated by distinct cell borders (Figure 5). The cytoplasm was usually clear or finely granular; however, a subset of tumor cells

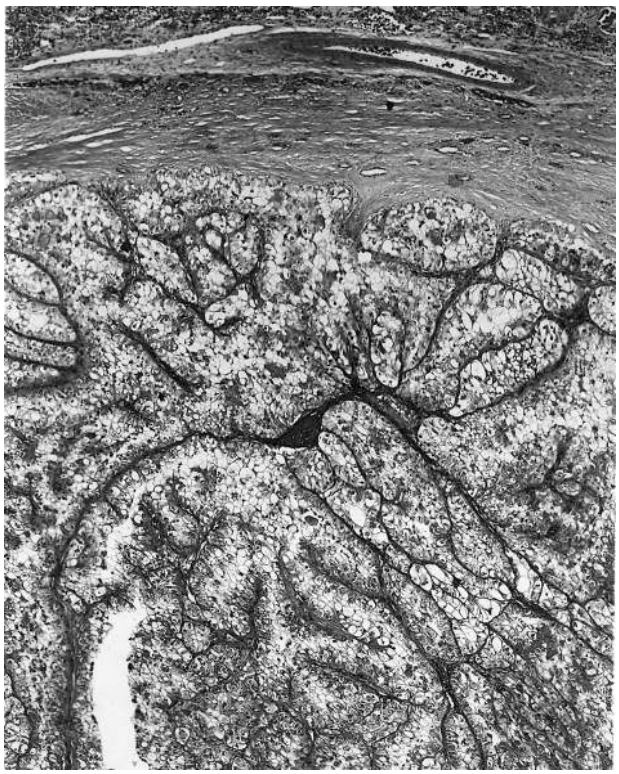

Figure 1. Low-power view of case 1 showing circumscription, nested, and pseudopapillary growth patterns (H&E; original magnification, ×100).

Table 1. Continued

Electron microscopy findings*	Cytogenetic t(X;17)	t(X;17) fusion transcripts by RT-PCR		17qter copy number by FISH	Follow-up
		ASPL-TFE3	*TFE3-ASPL*		
ASPS crystals, dense granules, CJ with lumens and microvilli, BM	t(X;17) (p11.2;q25)	Type 2	+	2	NED 4 years (no adjuvant therapy)
Dense granules, CJ, BM	t(X;17) (p11.2;q25)	Type 1	+	2	AWD 10 years
ND	Failed	Type 1	−	2	NED 7 years (no adjuvant therapy)
ND	der(X)t(X;7) (p11; p11), add(17) (q24–25)§	Type 1	−	2	NED 2.5 years
Dense granules, CJ	ND	Type 1	+	2	NED 13 months
Dense granules with early crystallization, rare CJ	ND	Type 1	+¶	2	DOD 2 years despite adjuvant therapy
Glycogen, fat, CJ with lumens and microvilli	ND	Type 1	−	ND	AWD (lung metastasis after 15 months)
Glycogen, fat, CJ with lumens and microvilli	ND	Type 1	+	2	NED 2 months

*, Dense granules refers to granules similar in size and shape to those seen in ASPS (see text).
†, Case previously reported as reference 7.
‡, Cases previously reported within reference 13.
§, Probable complex t(X;17), see text for complete karyotype.
¶, Out-of-frame fusion transcript (see text).
‖, Unresectable retroperitoneal metastasis.
f, focal; d, diffuse; CAM, cam5.2 antibody; CJ, cell junctions; BM, basement membrane material; ND, not done; AML, acute myelogenous leukemia; NED, no evidence of disease; DOD, died of disease; AWD, alive with disease; AJCC, American Joint Committee on Cancer, 1997 Revision; NWTS, National Wilms Tumor Study.

Figure 2. Low-power view of case 2 showing solid, sheet-like growth pattern where the alveolar septa do not connect (H&E; original magnification, ×100).

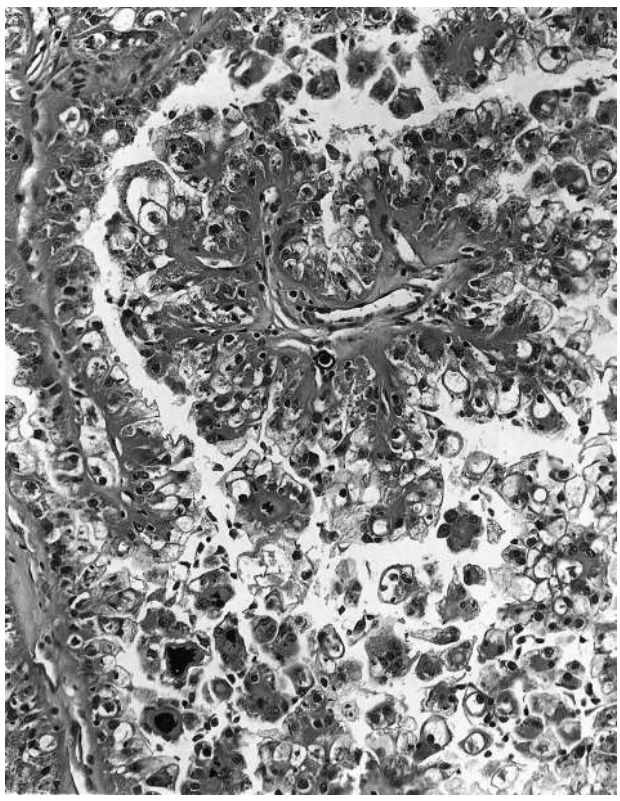

Figure 3. Intermediate-power view of case 1 showing pseudopapillary growth pattern and psammomatous calcification that occurs in hyaline cores of small pseudopapillae (H&E; original magnification, ×160).

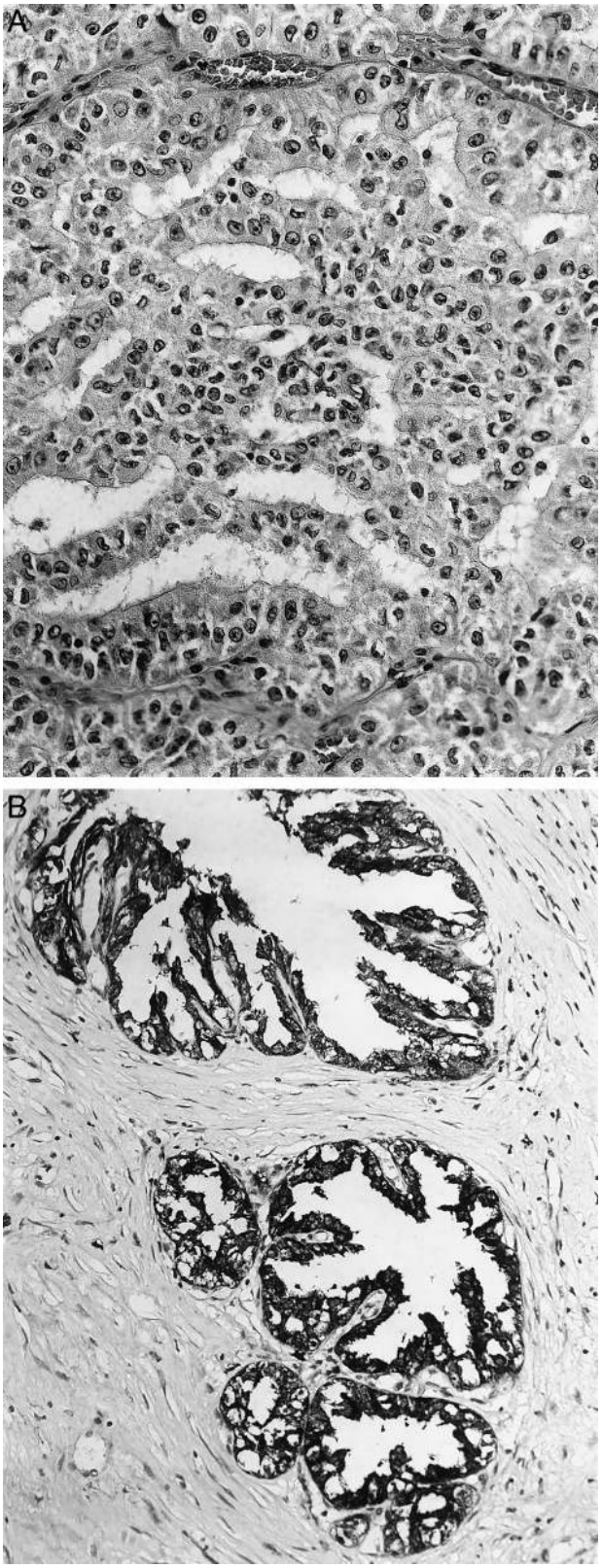

Figure 4. A: Trabecular growth pattern in case 6 (H&E; original magnification, ×160X). **B:** Diffuse EMA immunoreactivity in case 6 (DAKO Envision labeling; original magnification, ×160).

was densely granular and overtly eosinophilic. Larger, amphophilic cytoplasmic granules were also identified in

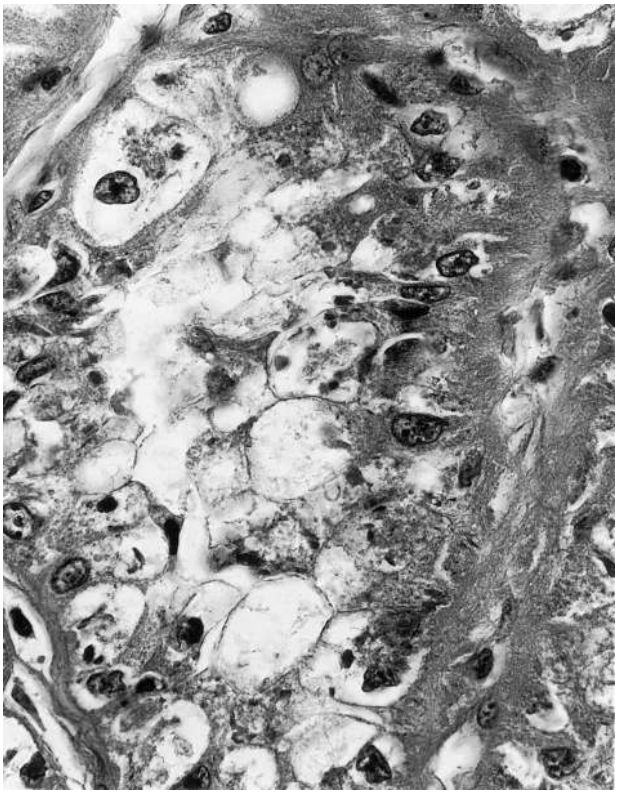

Figure 5. High-power view of case 1, showing fine and coarse cytoplasmic granularity, vesicular nuclei with prominent nucleoli (H&E; original magnification, ×630).

each case. Nuclei were eccentrically placed within the cells, and were somewhat rounded but had irregular borders on closer inspection. The chromatin was vesicular, with a single prominent nucleolus. Mitoses were extremely rare. In each tumor, periodic acid-Schiff (PAS) stains demonstrated fine granular cytoplasmic positivity that primarily disappeared with diastase treatment, consistent with glycogen. After diastase treatment, most of the tumors demonstrated scattered PAS-positive, diastase-resistant cytoplasmic granules; these were most prominent in case 4. However, none of the tumors demonstrated the well-formed PAS-positive, diastase-resistant intracytoplasmic crystals that are characteristic of ASPS.

These tumors tended to present at high stage. By NWTS-5 staging criteria, one tumor presented at stage 4 (because of bony metastasis), six at stage 3 (four because of lymph node metastasis, one because of piecemeal removal of tumor, one because of tumor unresectability), and one was stage 1. Using 1997 American Joint Committee on Cancer criteria, three tumors were stage IV, four tumors were stage III, and one tumor was stage I. All eight tumors demonstrated intrarenal vascular invasion. Perirenal (renal sinus) lymph nodes contained metastases in six of the seven cases in which nodes were identified on pathological examination.

Immunohistochemical Features

Vimentin highlighted the capillaries of the fibrovascular septa of all cases. Vimentin was negative in five of the

tumors, with only focal labeling of tumor cells in cases 4, 5, and 7. Cytokeratin antibody Cam5.2 labeled two tumors focally, whereas cytokeratin antibody AE1/3 labeled three tumors focally. Antibody to EMA focally labeled two of the latter tumors, and diffusely labeled another (case 6) that had shown prominent epithelial growth patterns (Figure 4B). The two tumors (cases 6 and 8) positive for EMA also labeled focally for S100 protein, whereas none of the other tumors did. The cytokeratin and EMA stains highlighted native renal tubules in contact with the nonreactive tumors, which emphasized their unencapsulated nature (Figure 6, A and B). None of the eight tumors labeled for desmin or HMB45.

Ultrastructural Features

Ultrastructural examination was performed on six cases, five on glutaraldehyde-fixed tissue, and a sixth on formalin-fixed, paraffin-embedded tissue. Four tumors demonstrated a distinctive combination of ASPS-like and epithelial features. These tumors all demonstrated abundant electron-dense granules that were similar in size and shape to those seen in ASPS and are not typical of any primary renal tumor. One of these four tumors, case 1, revealed well-formed rhomboid crystals, 270- to 276-nm wide in cross-section, composed of fibers with a periodicity of 10 nm and a diameter of 4.5 to 5.0 nm (Figure 7). These features are characteristic of the crystals of ASPS.[21] In one other case (case 6), partial or incipient crystallization typical of ASPS crystals was noted (Figure 8). However, each of the four cases also demonstrated abundant well-formed cell junctions, more than are typically seen in soft tissue ASPS, and suggestive of epithelial differentiation. Case 1 demonstrated more definitive epithelial differentiation, as it revealed prominent basement membrane, numerous cell junctions, and well-formed glandular lumens with microvilli (Figure 7). Case 1 therefore demonstrates features that are characteristic of ASPS and adenocarcinoma simultaneously. The two other tumors, cases 7 and 8, demonstrated features more typical of conventional RCC (intracellular glycogen, and fat, well-formed glandular lumens with microvilli) without the crystals or dense granules typical of ASPS.

Cytogenetic Features

The partial karyotype of case 1 is shown in Figure 9. The karyotype of case 2 has been previously reported.[7] Cytogenetic analysis was not performed in case 3, 5, 6, 7, or 8. Case 4 was previously reported in brief as showing a der(X)t(X;7)(p11;p11).[13] In fact, the initial karyotype was noted to be complex, and initially described as an 46,X,der(X)t(X;7)(p11;p12),del(1)(p34),add(1)(p34),+5,−6,add(7)(p11.2),+15, del(16)(p11.2),−17,add(20)(q13). Re-evaluation of this karyotype now suggests that it is better described as: 46,X,der(X)t (X;7)(p11;p11),del(1)(p34),add(1)(p34),+5,−6,add(7)(p11), del(16)(p11.2),add(17)(q24-25),add(20)(q13). Overall, this set of abnormal chromosomes could be explained by a complex t(X;17)(p11;q25), with translocation of Xp11 to 17q25, but of 17q25 to another chromosome. Thus, although nonreciprocal, the rearrangements in this case may nonetheless be genomically balanced in terms of chromosomes X and 17.

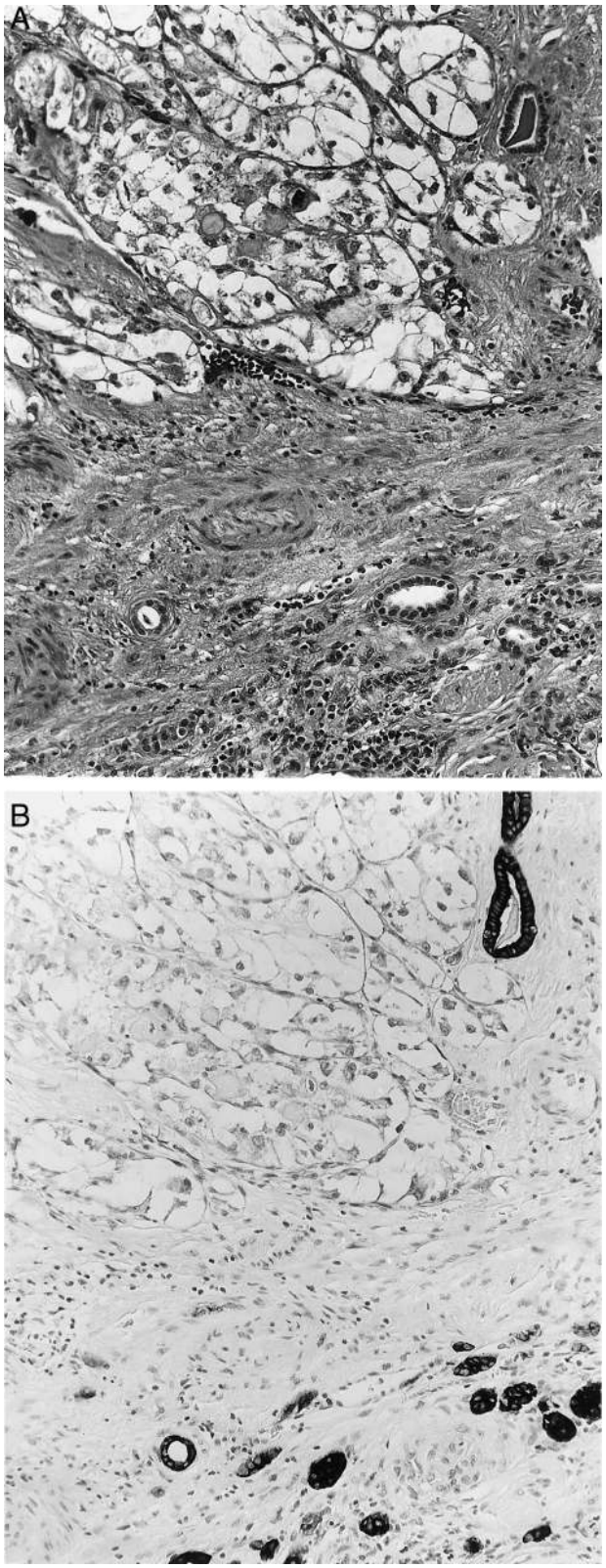

Figure 6. A: Unencapsulated tumor in case 1 abuts native renal tubules (H&E; original magnification, ×160). **B:** Cytokeratin AE1/AE3 labels native tubules, but not the tumor (avidin-biotin peroxidase; original magnification, × 160).

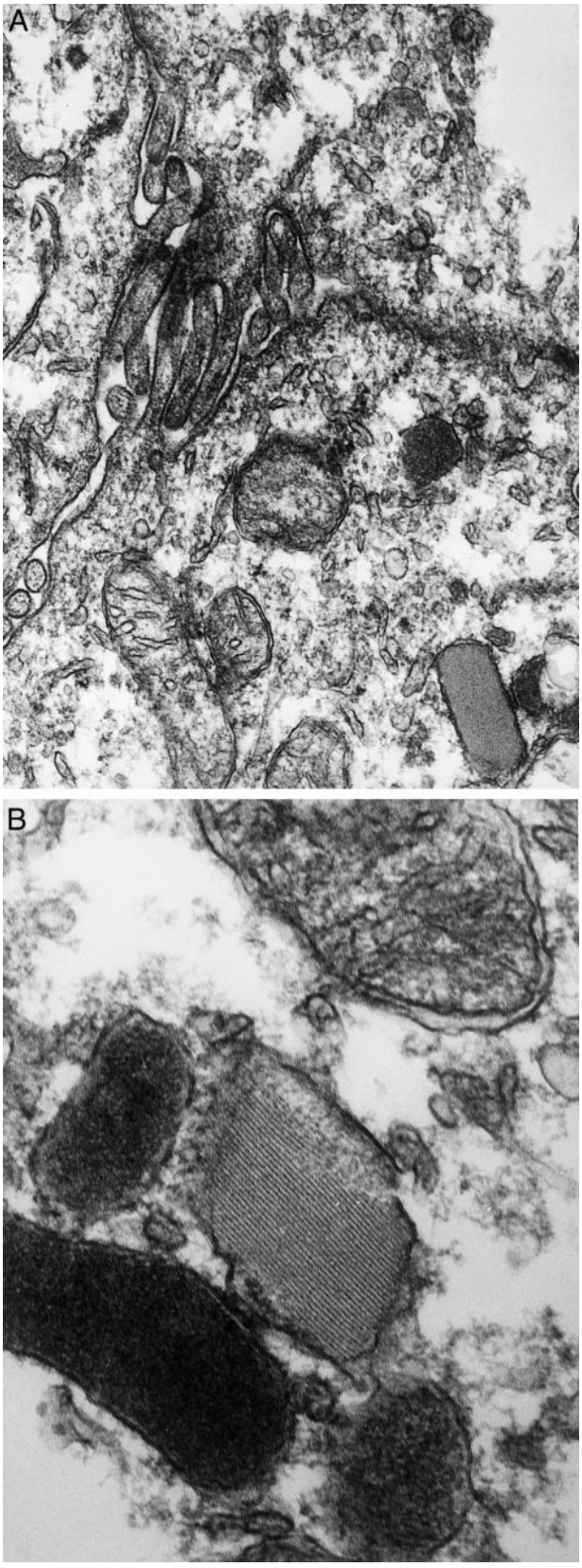

Figure 7. Case 1. **A:** Ultrastructural appearance of tumor cells showing an intercellular lumen with projecting slender microvilli. There is an intracytoplasmic membrane-bound crystal in the **lower-right corner** (original magnification, ×57,460). **B:** Detail of a membrane-bound rhomboid crystal from same case, composed of parallel rigid fibrils of 5-nm diameter and a periodicity of 10 nm, typical of ASPS crystals (original magnification, ×98,600).

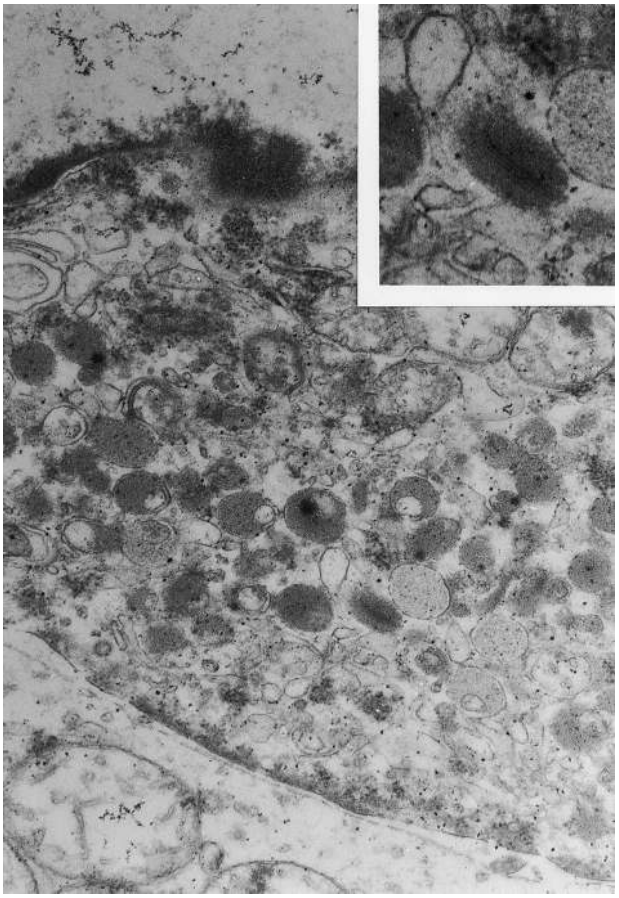

Figure 8. Case 6. Dense, membrane-bound cytoplasmic secretory granules (original magnification, ×36,400), similar to those seen in typical ASPS; **inset** shows detail of early crystallization of the secretory material in one of the granules, as in ASPS (see text) (original magnification, ×71,120).

The further molecular and FISH analyses in this case support this interpretation (see below).

Molecular Detection of the ASPL-TFE3 Fusion Transcript

RT-PCR performed on RNA extracted from frozen tumor (cases 1 to 3 and 5 to 8) or frozen short-term culture (case 4) identified a specific *ASPL-TFE3* fusion product in all eight cases, consistent with the presence of a t(X; 17)(p11.2;q25) (Figure 10). Two mutually exclusive types of *ASPL-TFE3* fusion transcripts were observed, corresponding to the two previously described types of *ASPL-TFE3* fusion transcripts. Cases 2 to 8 contained the type

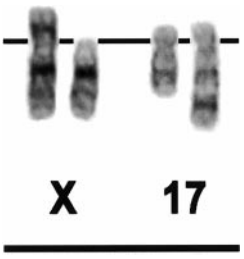

Figure 9. Partial karyotype of case 1 showing the t(X;17)(p11.2;q25).

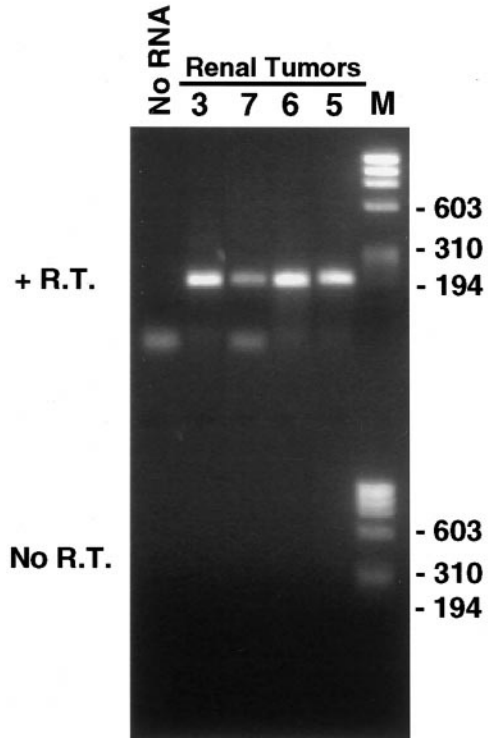

Figure 10. Detection of *ASPL-TFE3* fusion transcripts by RT-PCR. RT-PCR was performed as described in the text. The positive result (195-bp product) corresponding to the type 1 *ASPL-TFE3* fusion is seen in all four cases illustrated, and positive results were also obtained in the remaining four cases (not illustrated). Negative controls lacking RNA or containing sample RNA but lacking reverse transcriptase (no RT) were appropriately negative. M is the marker lane (*Hae*III digest of PhiX174 marker).

1 product, a fusion of *ASPL* to *TFE3* exon 4, whereas case 1 showed a type 2 product, a fusion of *ASPL* to *TFE3* exon 3. We tested seven other unrelated renal tumors (three clear cell carcinomas, two chromophobe carcinomas, one papillary carcinoma, one angiomyolipoma) as well as the K562 leukemia cell line by RT-PCR for *ASPL-TFE3* and they were all negative (results not shown).

Molecular Detection of the Reciprocal TFE3-ASPL Fusion Transcript

Because the t(X;17) in cases 1 and 2 appeared cytogenetically balanced, it should also lead to the formation of a *TFE3-ASPL* fusion gene. Therefore, we also tested all of the present cases for the reciprocal fusion product, *TFE3-ASPL*. Using appropriate *TFE3* forward and *ASPL* reverse primers (see Materials and Methods), we detected a *TFE3-ASPL* fusion transcript in five of eight cases (Figure 11 and Table 1), confirming that the rearrangement between the two genes was reciprocal in these cases. We performed direct sequencing of the *TFE3-ASPL* RT-PCR products to verify their fusion points. Cases 2, 5, and 8 showed the in-frame *TFE3* exon 3 to *ASPL* fusion expected from a reciprocal type 1 rearrangement (Figure 12). Case 1, which showed a type 2 rearrangement, also contained an in-frame *TFE3-ASPL* fusion transcript, but the *TFE3* fusion point was within *TFE3* exon 2 (Figure 12). Finally, case 6, which had a type 1 *ASPL-TFE3* fusion,

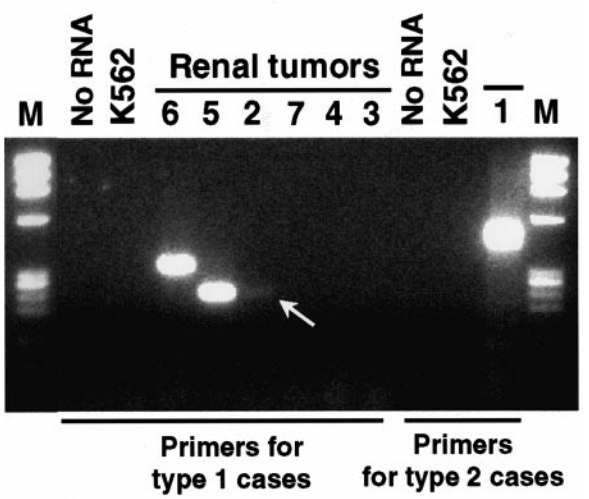

Figure 11. Detection of *TFE3-ASPL* fusion transcripts by RT-PCR. RT-PCR was performed as described in the text. Different primer combinations were used according to the type of *ASPL-TFE3* fusion detected in each tumor (see text). Positive results in four cases are illustrated (positive result in case 8 not shown). The product band in case 2 was faint (**arrow**). M is the marker lane (*Hae*III digest of PhiX174 marker). RT-PCR products were confirmed by sequencing. Partial sequences of the products are shown in Figure 12.

contained a reciprocal fusion in which a 113-nucleotide *ALU*-family-repeat sequence from approximately the midpoint of intron 3 of *TFE3* was inserted between *TFE3* exon 3 and *ASPL*, disrupting the reading frame (Figure 12), leading to premature termination within the portion encoded by the *ASPL*. This unusual product was not obtained when RT was omitted (result not shown), confirming that it was originating from cDNA and not

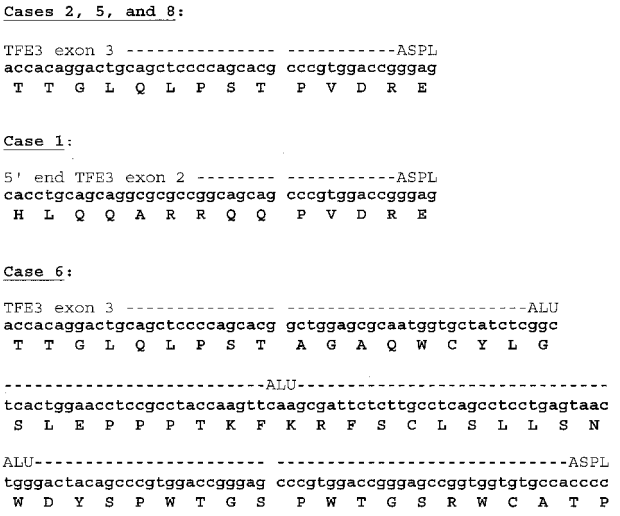

Figure 12. Partial sequences of fusion point of three types of reciprocal *TFE3-ASPL* fusion transcripts detected in individual renal tumors with the *ASPL-TFE3* fusion transcript. All eight tumors contained in-frame *ASPL-TFE3* fusion transcripts (see Results and Figure 10). The junction sequences of types 1 and 2 *ASPL-TFE3* fusion transcripts have been published elsewhere.[1] Five tumors also contained the reciprocal *TFE3-ASPL* fusion product (Figure 11), consistent with a simple reciprocal t(X;17)(p11;q25). The fusion transcripts in cases 1, 2, 5, and 8 were in frame and are predicted to encode a functional fusion protein. The transcript in case 6 contained an inserted *ALU* repeat sequence (see text), altering the reading frame of the *ASPL* portion of the transcript, which is otherwise identical to that in cases 1, 2, 5, and 8. This altered reading frame leads to premature termination within the portion encoded by *ASPL* (termination codon not shown).

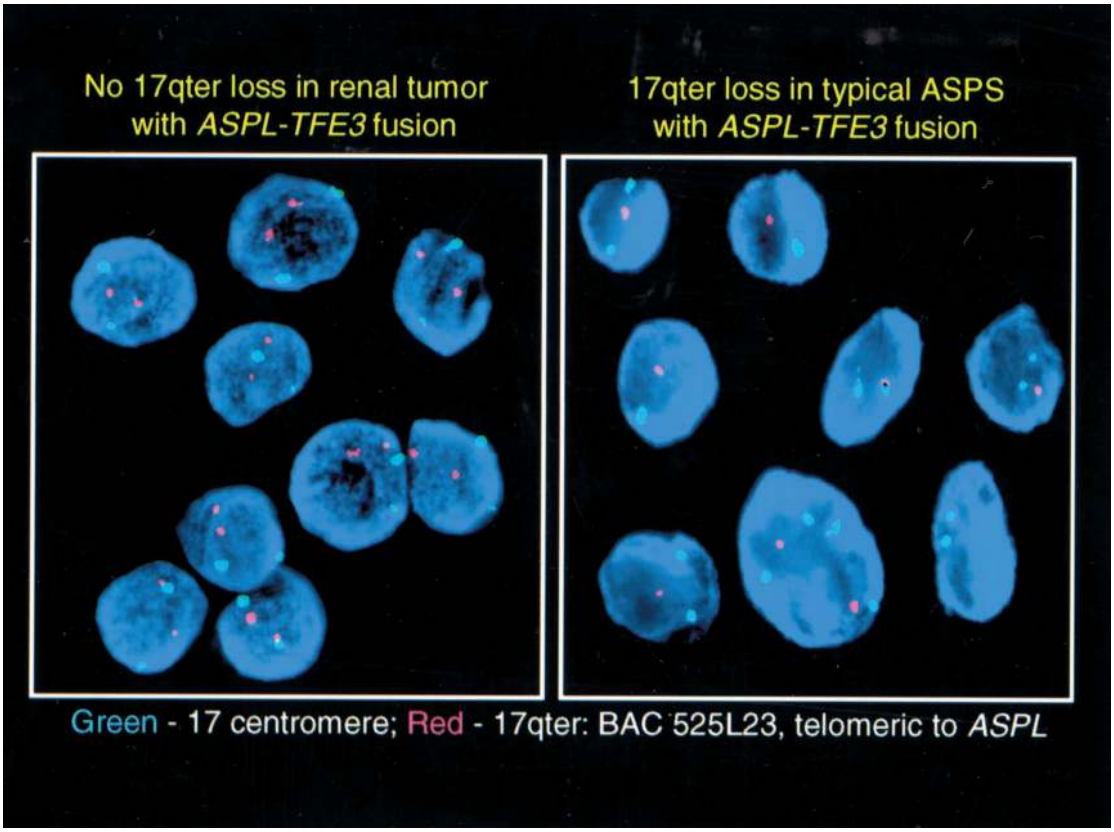

Figure 13. Bicolor interphase FISH analysis of copy number of 17qter distal to *ASPL*, to evaluate the balanced *versus* unbalanced nature of the t(X;17). Images shown are from a representative *ASPL-TFE3* renal tumor (case 1) and a representative ASPS case (case ASPS-2 from our previous study[1]). In these images, the 17qter probe [BAC 525L23 from 17q25.3, known to map telomeric to *ASPL* (see Materials and Methods)], appears red, whereas the centromere 17-specific probe, CEP 17, appears blue-green. The renal tumor cells show two green and two red signals throughout, as expected for a balanced t(X;17). In contrast, the ASPS cells show generalized loss of one red signal, as expected for an unbalanced t(X;17).

genomic DNA. Thus, although five of the eight cases showed evidence of expression of a *TFE3-ASPL* fusion transcript arising from a reciprocal rearrangement between *ASPL* and *TFE3*, only four of these cases contained in-frame *TFE3-ASPL* transcripts, capable of encoding potentially functional proteins.

FISH Analysis of 17q25.3 Copy Number Telomeric to ASPL

Although the presence of a *TFE3-ASPL* fusion gene could not be confirmed by RT-PCR in three of the eight cases (see above), we hypothesized that such cases may nonetheless contain a balanced rearrangement that is not leading to the expression of a *TFE3-ASPL* fusion RNA detectable by RT-PCR, either because the *TFE3-ASPL* fusion gene is not actively transcribed, or because they contain a more complex rearrangement (eg, three-way) that would produce an *ASPL-TFE3* fusion gene but not a *TFE3-ASPL* fusion gene. To test this hypothesis, we performed FISH to assess the copy number of the portion of 17q25.3 telomeric to the breakpoint in *ASPL*, reasoning that a balanced rearrangement (in the renal tumors) would result in retention of both copies of this region, whereas an unbalanced translocation (as in ASPS) would result in consistent loss of one copy. We used a bicolor FISH assay on interphase nuclei from frozen material available in seven of our renal cases, and in nine ASPS cases, using as a probe for 17q25.3 the BAC 525L23, known to map telomeric to *ASPL* (see Materials and Methods), in combination with the centromere 17-specific probe, CEP 17. All seven renal cases tested showed retention of both copies of BAC 525L23 (Table 1), whereas eight of nine ASPS showed loss of one copy (Figure 13). The seven renal cases tested included two of the three cases above in which no *TFE3-ASPL* fusion RNA was detected by RT-PCR. One of these two cases (case 4), had been karyotyped and in fact contained a more complex rearrangement (eg, three-way) that produced a *ASPL-TFE3* fusion gene but would not be expected to generate a *TFE3-ASPL* fusion gene. Thus, the cytogenetic, *ASPL-TFE3* RT-PCR, *TFE3-ASPL* RT-PCR, and FISH data in this case were entirely consistent with each other. The second of these two cases (case 3) had no cytogenetic data available, but the finding that both copies of BAC 525L23 were retained in this case, as well as all other cases tested, supports our hypothesis that the t(X;17) in these renal tumors is consistently genomically balanced, even if not necessarily simply reciprocal. Interestingly, the single case of ASPS without loss of BAC 525L23 was also the only case that we previously found to contain a *TFE3-ASPL* fusion transcript (case ASPS-7 from our

previous study[1]), further cross-validating the different approaches.

Clinical Follow-Up

Four patients (cases 1, 3, 4, and 5) are alive with no evidence of disease at 4 years, 7 years, 2.5 years, and 1.1 years, respectively. Of note, patients 1 and 3 are known to have not received any adjuvant therapy after surgery, whereas information regarding therapy is not available for patients 4 and 5. Patient 7 developed a pulmonary metastasis 15 months after surgery. Her unresectable retroperitoneal tumor showed no evidence of response to interleukin-2 therapy. Patient 2 is alive with stable retroperitoneal disease 12 years after surgery. Therapy with trimetrexate after the initial incomplete resection had stabilized the residual tumor, whereas α-interferon therapy did not have significant effect. Despite adjuvant chemotherapy, patient 6 died of progressive bony and lymph node metastases 2 years after surgery. At time of writing, patient 8 was newly diagnosed, with only 2 months of follow-up and no evidence of disease.

Discussion

We describe herein eight morphologically distinctive primary renal tumors of young patients that are genetically related to but distinct from soft tissue ASPS. All eight of these tumors had been initially classified as RCCs, as their morphology is consistent with that diagnosis. Retrospectively, we suspected that two of these tumors were genetically related to ASPS because they were characterized cytogenetically by the chromosome translocation, t(X;17)(p11.2;q25). An unbalanced chromosome translocation with cytogenetically identical breakpoints has been characterized recently as a hallmark of ASPS.[1] Prompted by the cytogenetic findings, we analyzed these renal tumors for the *ASPL-TFE3* fusion by RT-PCR. Indeed, *ASPL-TFE3* gene fusions were demonstrated in RNAs extracted from frozen material from each of the eight renal tumors. However, using FISH probes for the centromere and long arm telomere of chromosome 17 and RT-PCR for the chimeric RNA encoded by a reciprocal *TFE3-ASPL* fusion gene, we were able to document a unique and intriguing distinction between the t(X;17) in these renal tumors and in soft tissue ASPS. The t(X;17) translocation proved to be balanced in all seven renal tumors tested, in sharp contrast to soft tissue ASPS where we demonstrate it to be unbalanced in eight of nine cases. This distinction was already suggested by a perusal of existing cytogenetic case reports on these renal tumors, but its consistency was not yet apparent.

It is difficult to place these neoplasms within an existing well-defined category, because they demonstrate individual features characteristic of both ASPS and RCC. These features seem to be variably developed in the different cases. The presence of the *ASPL-TFE3* gene fusion and the ultrastructural identification of the characteristic membrane-bound crystals in case 1 are further evidence for a relationship to ASPS. With regards to the latter, we note that, contrary to what is generally assumed, classic intracytoplasmic crystals[22] are not found in most soft tissue ASPS. Rather, ASPS often contain electron-dense granules consisting of finely filamentous material (termed "precrystalline" by some).[22,23] Three of the other renal tumors in this series contained dense granules of this type, some with early crystallization. Because well-formed crystals seem to be rare in these tumors, it is perhaps not surprising that they were not identified in the single section from case 1 stained with PAS-diastase. Finally, the tendency of the *ASPL-TFE3* renal tumors to present at high stage is also reminiscent of the behavior of ASPS, as is the indolent clinical course experienced by patient 2.

However, aside from their renal location, these tumors demonstrate several features that are more typical of RCC than of soft tissue ASPS. First, these renal tumors frequently spread to lymph nodes, which are commonly involved by RCC only rarely involved by usual soft tissue ASPS.[9–12] Second, the consistent presence of psammoma bodies, clear cell cytology, and pseudopapillary architecture give these lesions an appearance that is

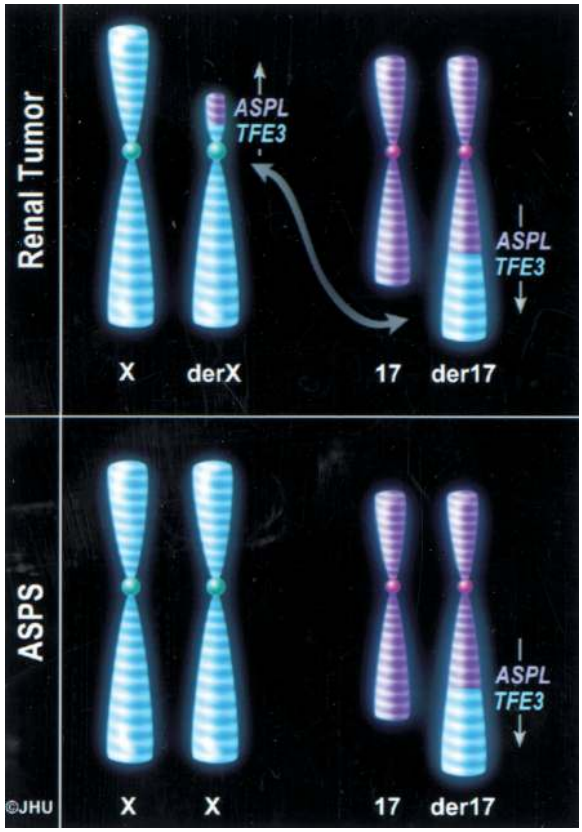

Figure 14. Schematic representation of the differences between the unbalanced der(17)t(X;17)(p11.2;q25) of soft tissue ASPS and the balanced translocation identified in the t(X;17)(p11.2;q25) renal tumors. Both translocations are shown occurring in a 46, XX female in this illustration. Chromosome X material is colored green, whereas chromosome 17 material is colored purple. Whereas soft tissue ASPS has an extra copy of the majority of the short arm of the X chromosome (distal to Xp11.2) and is missing one copy of the small amount of chromosome 17 that is telomeric to 17q25, the *ASPL-TFE3* renal tumors show neither loss nor gain of genetic material at these loci. The locations of the *ASPL-TFE3* and *TFE3-ASPL* fusion genes are shown and their orientation is indicated by the **arrows** (artwork by Jennifer L. Parsons, M. A.).

Table 2. Additional Probable Renal *ASPL-TFE3* Tumors Previously Reported as Pediatric Renal Cell Carcinomas

Reference	Age/sex	Diameter/stage	Immuno-histochemistry	Cytogenetics	Microscopic description in report
Hernandez-Marti et al[6]	8/M	3.5 cm, stage 3 (lymph node)	Not reported	t(X;17)(p11.2;q25)	"Tubular and papillary tumor composed of large clear cells. Their cytoplasm was often foamy."
Carcao et al[5]	6/F	Unknown, stage 3 (lymph node)	Not reported	t(X;17)(p11.2;q25) t(1;12)	"clear cell"
Heimann et al[8]	NA	NA	Not reported	t(X;17)(p11;q25)	"clear cell"

NA, not available.

distinct from soft tissue ASPS and highly suggestive of carcinoma. Along these lines, only rare soft tissue ASPS have been reported to contain psammomatous calcifications,[24,25] and most are composed of eosinophilic cells in well-defined nests.[26] Third, a higher percentage (four of eight, or 50%) of *ASPL-TFE3* renal tumors than soft tissue ASPS (4%) labeled, albeit focally, for cytokeratin, which is present in >85% of RCCs.[12] Finally, three of the *ASPL-TFE3* renal tumors (cases 1, 7, and 8) did show definitive evidence of epithelial differentiation on ultrastructural analysis. Interestingly, two of these cases (cases 1 and 7) showed no evidence of cytokeratin expression immunohistochemically. Despite these findings, however, we note that in the majority of these tumors, epithelial features are not fully developed. This view is supported by the finding of only abortive epithelial differentiation ultrastructurally in the form of prominent cell junctions (which alone is not conclusive proof of carcinoma) in four cases, and the relatively low percentage of cases that label for cytokeratin compared to RCC. Moreover, even the cytokeratin-positive cases demonstrated only focal labeling of individual cells despite the application of a broad panel of anti-cytokeratin reagents. Hence, we cannot consider these tumors to be typical carcinomas, particularly in light of the above features that also link them to ASPS.

We suspect that the differences between soft tissue ASPS and these renal tumors is related to the structure of the t(X;17)(p11.2;q25). Most chromosome translocations are usually reciprocal, resulting in two opposite fusion genes, one on each of the two derivative chromosomes, with no net gain or loss of genetic material.[27] The reciprocal fusion gene is sometimes also transcribed although the encoded reciprocal fusion protein is rarely functionally significant. The t(X;17)(p11.2;q25) of soft tissue ASPS is peculiar insofar as it appears unbalanced in most cases analyzed cytogenetically, an observation now supported by our recent molecular studies in which the reciprocal *TFE3-ASPL* transcripts were found in only 1 of 13 cases tested[1] (including case ASPS-13) and by the current FISH study showing retention of both copies of 17q25.3 telomeric to *ASPL* in only one of nine ASPS cases (the same case was the exception by both methods). Thus, the *ASPL-TFE3* fusion of soft tissue ASPS is associated in almost all cases with allelic loss at 17q25.3 telomeric to *ASPL* (and gain of Xp sequences telomeric to *TFE3*) (Figure 14). The additional chromosome X material includes most of the short arm. The possible additional role of these recurrent translocation-associated genomic imbalances in the biology of soft tissue ASPS is unknown.

In contrast, the t(X;17)(p11.2;q25) in the renal tumors described herein was cytogenetically balanced in six of six cases with karyotypic data, including cases 1, 2, and 4 in the present series and three additional published cases (see below and Table 2). We confirmed the balanced nature of the translocation in all seven cases tested by FISH in this series. This was also supported by our demonstration of the reciprocal fusion product, *TFE3-ASPL*, in five cases. The negative RT-PCR result in case 4 was expected given the cytogenetically identified complex rearrangement that was nonreciprocal (but balanced in terms of 17q25.3 copy number). The negative

Table 3. Translocation-Associated Neoplasms Confirmed Molecularly as Primary Renal Tumors

Tumor	Translocation	Reference
Ewing sarcoma/peripheral primitive neuroectodermal tumor	t(11;22)(q24;q12)	Quezado et al[31], Parham et al[32]
Synovial sarcoma (classic embryonal sarcoma of the kidney)	t(X;18)(p11;q11)	Argani et al[33]
Infantile fibrosarcoma (cellular congenital mesoblastic nephroma)	t(12;15)(p13;q25)	Rubin et al[34], Knezevich et al[35]
Clear cell sarcoma of soft parts (malignant melanoma of soft parts)	t(12;22)(q13;q12)	Rubin et al[36]
Alveolar rhabdomyosarcoma	t(1;13)(q36;q14) or t(2;13)(q35;q14)	F. Barr, M. K. Fritsch, P. Argani,* unpublished observations
ASPL-TFE3 tumors related to alveolar soft part sarcoma	t(X;17)(p11.2;q25)	Current report

* *PAX-FKHR* fusion was not further subtyped in this case.

TFE3-ASPL RT-PCR result in case 7 does not exclude a balanced rearrangement because the reciprocal fusion gene may not necessarily be transcribed in all cases, as we speculate may have happened in case 3.

Thus, it seems that unlike ASPS, the present renal tumors are not associated with any consistent loss or gain of genetic material from the rearranged chromosomes. The finding of distinctive tumors being associated with balanced and unbalanced forms of the same translocation is, to our knowledge, entirely novel. A re-examination of other translocations in light of this unexpected observation may be warranted. Perhaps the differences in gene dosage or the presence of a functional *TFE3-ASPL* fusion product (in some cases) account for the differing morphology and pattern of spread of these renal tumors. Another possibility is a role for the loss of the only functional copy of *TFE3* in these renal tumors (but not in ASPS), given that *TFE3* is subject to X-inactivation[28] and assuming that the t(X;17) in females are involving the active X. Alternate hypotheses are that the clinicopathological differences reflect (i.e., a renal tubular cell versus a primitive mesenchymal cell of soft tissue) differences between the renal and soft tissue precursor cells in which the t(X;17) occurs, and/or the local effects of the renal environment on the tumor. In support of the latter hypothesis, other primary renal sarcomas such as clear cell sarcoma of the kidney frequently spread to renal hilar lymph nodes,[29] perhaps because of the rich lymphatic drainage system inherent to the kidney. Also, the consistent calcifications in these tumors may relate to the prominent role the renal parenchyma plays in transporting calcium to preserve it from urinary wastage. Regardless, given the significant genetic and histopathological differences between the *ASPL-TFE3* renal tumors and soft tissue ASPS, we consider these neoplasms to be distinctive entities.

As previously mentioned, we note three additional renal tumors (aside from case 2 of this series), reported as carcinomas in the literature, that demonstrated a cytogenetically balanced t(X;17)(p11.2;q25) in each case (Table 2). None of these tumors were illustrated nor were any immunohistochemical stains reported. Two of the tumors presented with lymph node metastasis, consistent with the trend in our series. All of these tumors had clear cell morphology. We strongly suspect that these represent additional examples of the presently described entity. Interestingly, it has long been noted that pediatric renal cell carcinomas are often nonimmunoreactive for cytokeratins, although an explanation has not been evident. It is likely that some of those cytokeratin-negative carcinomas are additional examples of these *ASPL-TFE3* tumors.

Although the renal tumors we report all occurred in patients younger than 20 years of age, our experience is somewhat biased toward pediatric renal tumors given the nature of the NWTSPC. We note that soft tissue ASPS affects a broader age range than the lesions we have identified in the kidney. Although ASPS is typically a tumor of children and young adults, the 0 to 20 year age range that encompasses our renal tumors accounts for only 37% of ASPS cases.[12] This suggests that additional cases of primary renal *ASPL-TFE3* lesions could be found among adult renal tumors, perhaps among the 6 to 7% of unclassifiable carcinomas or among tumors classified as conventional (clear cell) or papillary carcinoma, particularly those that are cytokeratin-negative.[30] However, two lines of evidence suggest that the *ASPL-TFE3* renal tumors preferentially affect young patients. First, the renal tumors reviewed at MSKCC were not biased toward young patients; in fact, they were predominantly from adults. The *ASPL-TFE3* tumors identified within this group were identified purely on morphological grounds without knowledge of the patients' ages, and they proved to be from the minority of tumors resected from young patients. Second, on review of the online Chromosomes Aberration Database (http://www.ncbi.nlm.nih.gov.), we note that of 667 renal carcinomas with published abnormal karyotypes, three have demonstrated the t(X;17)(p11.2;q25). All of these tumors were in individuals younger than 10 years of age, whereas more than 95% of the whole group were adults.

Finally, we again note the predilection of translocations that classically are associated with soft tissue tumors to occur in primary renal tumors[31–36] (Table 3). With the exception of infantile fibrosarcoma, clear cell sarcoma of soft parts, and these *ASPL-TFE3* renal tumors, all of the other tumors were previously usually considered to be Wilms tumor variants before molecular analysis allowed their definitive distinction. Separation of these entities from Wilms tumor has allowed the clinical behavior of the latter to be better understood. Distinction of primary renal *ASPL-TFE3* tumors from true pediatric RCCs should help allow us to better understand the clinicopathological features of both, which should lead to more appropriate management approaches.

Acknowledgments

We thank Selva Murugesan for performing the immunohistochemical stains; Ann Baren and Elizabeth Weiss for technical support with the ultrastructural examination; Stanley Matthews and Kelli Geppi for assistance with shipping; Norman Barker and Kin Chung Kong for expert photographic assistance; Theresa Cantone and Lucy Wangaruro for excellent secretarial support; Dr. Jean M. Henneberry for providing slides from case 7; Dr. David Gang for providing material for ultrastructural examination from case 7; Dr. J. T. Mascarello for providing the karyotype from case 1; and William L. Gerald M.D. Ph.D., Jonathan I. Epstein M.D., and Elizabeth A. Montgomery, M.D. for helpful discussions.

References

1. Ladanyi M, Lui MY, Antonescu CR, Krause-Boehm A, Meindl A, Argani P, Healey JH, Ueda T, Yoshikawa H, Meloni-Ehrig A, Sorensen PHB, Mertens F, Mandahl N, van den Berghe H, Sciot R, Dal Cin P, Bridge J: The der(17)t(X;17)(p11;q25) of human alveolar soft part sarcoma fuses the TFE3 transcription factor gene to ASPL, a novel gene at 17q25. Oncogene 2001, 20:48–57
2. Sidhar SK, Clark J, Gill S, Hamoudi R, Crew AJ, Gwilliam R, Ross M, Linehan WM, Birdsall S, Shipley J, Cooper C: The t(X;1) (p11.2;q21.2)

translocation in papillary RCC fuses a novel gene PRCC to the TFE3 transcription factor gene. Hum Mol Genet 1996, 5:1333–1338
3. Weterman MAJ, Wilbrink M, van Kessel AG: Fusion of the transcription factor TFE3 gene to a novel gene, PRCC, in t(X;1)(p11.2;q21)-positive papillary RCCs. Proc Natl Acad Sci USA 1996, 93:15294–15298
4. Clark J, Lu Y-J, Sidhar SK, Parker C, Gill S, Smedley D, Hamoudi R, Linehan WM, Shipley J, Cooper CS: Fusion of splicing factor genes PSF and NonO (p54nrb) to the TFE3 gene in papillary RCC. Oncogene 1997, 15:2233–2239
5. Carcao MD, Taylor GP, Greenberg ML, Bernstein ML, Champagne M, Hershon L, Baruchel S: Renal cell carcinoma in children. A different disorder from its adult counterpart? Med Pediatr Oncol 1998, 31:153–158
6. Hernandez-Marti MJ, Orellana-Alonso C, Badia-Garrabou L, Miralles AV, Paradis-Alos A: Renal adenocarcinoma in an 8-year-old child, with a t(X;17)(p11.2;q25). Cancer Genet Cytogenet 1995, 83:82–83
7. Tomlinson GE, Nisen PD, Timmons CF, Schneider NR: Cytogenetics of a RCC in a 17-month-old child. Evidence for Xp11.2 as a recurring breakpoint. Cancer Genet Cytogenet 1991, 57:11–17
8. Heimann P, Devalck C, Debusscher C, Sariban E, Vamos E: Alveolar soft-part sarcoma. Further evidence by FISH for the involvement of chromosome band 17q25. Genes Chromosom Cancer 1998, 23:194–197
9. Auerbach HE, Brooks JJ: Alveolar soft part sarcoma. A clinicopathologic and immunohistochemical study. Cancer 1987, 60:66–73
10. Christopherson WM, Foote FW, Stewart FW: Alveolar soft part sarcomas. Structurally characteristic tumors of uncertain histogenesis. Cancer 1952, 5:100–111
11. Lieberman PH, Brennan MF, Kimmel M, Erlandson RA, Garin-Chesa P, Flehinger BY: Alveolar soft part sarcoma. A clinico-pathologic study of half a century. Cancer 1989, 63:1–13
12. Ordonez NG: Alveolar soft part sarcoma: a review and update. Adv Anat Pathol 1999, 6:125–139
13. Renshaw AA, Granter SR, Fletcher JA, Kozakewich HP, Corless CL, Perez-Atayde AR: Renal cell carcinomas in children and young adults: increased incidence of papillary architecture and unique subtypes. Am J Surg Pathol 1999, 23:795–802
14. Miller RT: Immunohistochemistry of epithelial tumors: metastatic carcinoma of unknown origin, hepatoma, and mesothelioma. American Society of Clinical Pathologists 1999 Fall Meeting, New Orleans, LA, Workshop #A176 Syllabus, September 25, 1999
15. DeYoung BR, Wick MR: Immunohistologic evaluation of metastatic carcinomas of unknown origin: an algorhythmic approach. Semin Diagn Pathol 2000, 17:184–193
16. Miettinen M: Keratin immunohistochemistry: update of applications and pitfalls. Pathol Annu 1993, 28:113–143
17. Renshaw AA, Zhang H, Corless CL, Fletcher JA, Pins MR: Solid variants of papillary (chromophil) RCC: clinicopathologic and genetic features. Am J Surg Pathol 1997, 21:1203–1209
18. Chomcyznski P, Sacchi N: Single step method of RNA isolation by acid-guanidinium thiocyanate-phenol-chloroform extraction. Anal Biochem 1987, 162:156–159
19. Argani P, Perez-Ordonez B, Xiao H, Caruana SM, Huvos AG, Ladanyi M: Olfactory neuroblastoma is not related to the Ewing family of tumors. Absence of EWS/FLI1 gene fusion and MIC2 expression. Am J Surg Pathol 1998, 22:391–398
20. Murphy WM, Beckwith JB, Farrow GM: Tumors of the kidney, bladder, and related urinary structures. Atlas of Tumor Pathology, Third Series, Fascicle 11. Washington, DC, Armed Forces Institute of Pathology, 1993, pp 102–104
21. Erlandson RA: Diagnostic Transmission Electron Microscopy of Tumors. New York, Raven Press, 1994, pp 270–274
22. Tucker JA: Crystal-deficient alveolar soft part sarcoma. Ultrastructural Pathology 1993, 17:279–286
23. Menesce LP, Eyden BP, Edmondson D, Harris M: Immunophenotype and ultrastructure of alveolar soft part sarcoma. J Submicrosc Cytol Pathol 1993, 25:377–387
24. Chetty R: Alveolar soft part sarcoma with psammoma bodies. Histopathology 1990, 17:188
25. Persson S, Willems J-S, Kindblom L-G, Angervall L: Alveolar soft part sarcoma. An immunohistochemical, cytologic, and electron-microscopic study and a quantitative DNA analysis. Virchows Archiv A Pathol Anat Histopathology 1998, 412:499–513
26. Enzinger FM, Weiss SW: Soft Tissue Tumors. St. Louis, Mosby, 1995
27. Ladanyi M, Bridge JA: Contribution of molecular genetic data to the classification of sarcomas. Hum Pathol 2000, 31:532–538
28. Carrel L, Cottle AA, Goglin KC, Willard HF: A first-generation X-inactivation profile of the human X chromosome. Proc Natl Acad Sci USA 1999, 96:14440–14444
29. Argani P, Perlman EJ, Breslow NE, Browning NG, Green DM, D'Angio GJ, Beckwith JB: Clear cell sarcoma of the kidney: a review of 351 cases from the National Wilms Tumor Study Group Pathology Center. Am J Surg Pathol 2000, 24:4–18
30. Reuter VE, Presti JC: Contemporary approach to the classification of renal epithelial tumors. Semin Oncol 2000, 27:124–137
31. Quezado M, Benjamin DR, Tsokos M: EWS/FLI-1 fusion transcripts in three peripheral primitive neuroectodermal tumors of the kidney. Hum Pathol 1997, 28:767–771
32. Parham DM, Roloson GJ, Feely M, Green DM, Bridge JA, Beckwith JB: Primary malignant neuroepithelial tumors of the kidney. A clinicopathologic analysis of 146 adult and pediatric cases from the National Wilms Tumor Study Group Pathology Center. Am J Surg Pathol 2001, 25:133–146
33. Argani P, Faria PA, Epstein JI, Reuter VE, Perlman EJ, Beckwith JB, Ladanyi M: Primary renal synovial sarcoma. Morphologic and molecular delineation of an entity previously included among embryonal sarcomas of the kidney. Am J Surg Pathol 2000, 24:1087–1096
34. Rubin BP, Chen CJ, Morgan TW, Xiao S, Grier HE, Kozakewich HP, Perez-Atayde AR, Fletcher JA: Congenital mesoblastic nephroma t(12;15) is associated with the ETV6-NTRK3 gene fusion: cytogenetic and molecular relationship to congenital (infantile) fibrosarcoma. Am J Pathol 1998, 153:1451–1458
35. Knezevich SR, Garnett MJ, Pysher TJ, Beckwith JB, Grundy PE, Sorensen PH: ETV6-NTRK3 gene fusions and trisomy 11 establish a histogenetic link between mesoblastic nephroma and congenital fibrosarcoma. Cancer Res 1998, 58:5046–5048
36. Rubin BP, Fletcher JA, Renshaw AA: Clear cell sarcoma of soft parts: report of a case primary in the kidney with cytogenetic confirmation. Am J Surg Pathol 1999, 23:589–594